3032–3038 *Nucleic Acids Research, 2007, Vol. 35, No. 9* *Published online 16 April 2007*
doi:10.1093/nar/gkm199

The open state of human topoisomerase I as probed by molecular dynamics simulation

Giovanni Chillemi[1], Alessandro Bruselles[2], Paola Fiorani[2], Susana Bueno[1] and Alessandro Desideri[2,*]

[1]CASPUR Inter-University Consortium for the Application of Super-Computing for Universities and Research, Via dei Tizii 6, Rome 00185, Italy and [2]INFM National Institute for the Physics of Matter, interdisciplinary Centre of Bioinformatics and Biostatistics and Department of Biology, University of Rome Tor Vergata, Via Della Ricerca Scientifica, Rome 00133, Italy

Received February 23, 2007; Revised March 20, 2007; Accepted March 21, 2007

ABSTRACT

The open state of human topoisomerase I has been probed by molecular dynamics simulation, starting from the coordinates of the closed structure of the protein complexed with DNA, after elimination of the 22-bp DNA duplex oligonucleotide. A repulsion force between the two lips of the protein has been introduced for a short time to induce destabilization of the local minimum, after which an unperturbed simulation has been carried out for 10 ns. The simulation shows that the protein undergoes a large conformational change due to rearrangements in the orientation of the protein domains, which however move as a coherent unit, fully maintaining their secondary and tertiary structures. Despite movements between the domains as large as 80–90 Å, the catalytic pentad remains preassembled, the largest deviation of the active site backbone atoms from the starting crystallographic structure being only 1.7 Å. Electrostatic calculation of the open protein structure shows that the protein displays a vast positive region with the active site residues located nearly at its center, in a conformation perfectly suited to interact with the negatively charged supercoiled DNA substrate.

INTRODUCTION

Eukaryotic topoisomerase I is a monomeric enzyme that catalyzes the relaxation of supercoiled DNA during important processes including DNA replication, transcription, recombination and chromosome condensation (1–3). Human topoisomerase I (hTop1) is composed of 765 amino acids, and proteolytic experiments have shown that the enzyme is composed of four different domains: N-terminal domain (residues 1–214), core domain (residues 215–635), linker domain (residues 636–712), and C-terminal domain (residues 713–765) (4). The 3D structure of the enzyme without the N-terminal domain (topo70), complexed with a linear double-helix DNA substrate, has permitted a further classification of the core domain in subdomain I (residues 215–232 and 320–433), II (residues 233–319) and III (residues 434–635), and has shown that topoisomerase I is a bi-lobed protein that clamps completely around duplex DNA through protein–DNA phosphate interaction (5,6). One lobe is constituted by the C-terminal catalytic domain and core subdomain III, the other one (called 'cap') by core subdomains I and II. The protein forms a substantially closed clamp between loops, designated lip1 and lip2, belonging to core subdomains I and III, respectively. The two lips interact directly through a non-covalent interaction between the carboxylic lateral group of Glu497 and the side-chain amino group of Lys369 (5).

The catalytic cycle of the enzyme is composed of five steps: DNA association, cleavage, strand rotation, ligation and dissociation (6). A complete understanding of the DNA recognition event and the conformational changes that follow DNA binding would require determination of the 3D structure of the enzyme in the free and DNA-bound states. Large domain movements are required for the protein to bind the supercoiled DNA substrate, likely through the flexible hinge that has been hypothesized to be located between the 'cap' and subdomain III (helices 8 and 9) (5). Indeed a molecular dynamics (MD) simulation study suggested the occurrence of a movement of ~10–14 Å between the lips, during the DNA rotation step (7). Two articles have demonstrated that introduction of two cysteines on the two lips, by site-directed mutagenesis, traps hTop1 in the closed conformation, through a disulfide bridge upon DNA addition, confirming the existence of ample conformational changes (8,9). Until now, the structure of the protein has been solved only in the closed form, when it is fully embracing the DNA, and no information is available

*To whom correspondence should be addressed. Tel: +39 0672594376; Fax: +39 062022798; Email: desideri@uniroma2.it

concerning the preferred conformation in the absence of the substrate.

A paper describing the open state of the topoisomerase IB from *Deinococcus radiodurans* has recently appeared (10). The bacterial enzyme is much smaller than the human one, being constituted by a C-terminal domain of about 250 residues, comparable to the core subdomain III and C-terminal domain of the human enzyme, and by an N-terminal domain of about 90 residues that has no counterpart in the human enzyme. The two domains are splayed apart in an open conformation in which the surface of the catalytic domain containing the active site is exposed for DNA binding. In the case of the human enzyme, the internal flexibility of the protein in the absence of DNA, and the consequent conformational heterogeneity, makes its crystallization and analysis through X-ray diffraction very difficult. Therefore, different methods must be applied.

MD simulation is a powerful technique that is widely used to probe the flexibility of proteins, DNA, and protein–DNA complexes, and also has been used to examine the properties of DNA-topoisomerase I complexes (11–14). Starting from the hTop1 closed crystallographic structure, the flexibility of the different domains have been monitored, but it has not been possible to monitor the so-called open state conformation, because of the strict non-covalent interactions occurring between the protein domains and DNA (11). MD can also be applied to sample large conformational changes after introducing a perturbation or a force that imposes the system to sample events occurring on a timescale not accessible by the current computational resources. This approach has been used to study the conformational changes of several proteins (15,16), and to propose a model for the relaxation of positive and negative DNA supercoils in the hTop1–DNA complex (7).

In this work, we have carried out a simulation of the human topoisomerase enzyme, starting from the closed configuration coordinates of the topo70-DNA non-covalent complex after elimination of the 22-bp DNA duplex oligonucleotide coordinates. A repulsion force between the two lips has been introduced for a short time to induce the destabilization of the local minimum, and then an unperturbed simulation was carried out for 10 ns. Analysis indicates the occurrence of a large reorientation of the different domains that however, fully maintain their secondary and tertiary structures. Beside such a large conformational change, which induces movements as large as 80–90 Å between the domains, the active site residues remain preassembled, and the open structure of the protein displays a vast positive region with the active site located nearly at its center, perfectly suited to interact with the negatively charged DNA substrate.

METHODS

The initial configuration of hTop1 was modeled obtaining the starting position for residues 215–633 and 641–765 from the crystal structure 1a36 (6), and those for residues 203–214 from the crystal structure 1ej9 (17). The seven residues constituting the loop region that connects the linker to the core domain (residues 634–640, which are lacking in the 1a36 PDB structure because of thermal fluctuation) were added to the system by molecular modeling, as already described (14), using the SYBYL program (St Louis, MO). The same procedure has been followed to reconstruct the partially missing side chains of the residues not fully detected in the X-ray diffraction structure. The spatial environment of each new residue was checked for close contact or overlap with neighboring residues, and stereochemical regularization of the structures was obtained by the Powell minimization method implemented in the SYBYL program.

The system was modeled with the AMBER95 all-atom force field (18), and placed in a rectangular box ($111 \times 152 \times 133$ Å^3) filled with TIP3P water molecules (19). The dimension of the box was sufficiently large to accommodate the protein also in the open state, without any interactions with its periodic images. The system was, in fact, simulated in periodic boundary conditions, using a cutoff radius of 9 Å for the non-bonded interactions, and updating the neighbor pair list every 10 steps. The electrostatic interactions were calculated with the Particle Mesh Ewald method (20,21). The SHAKE algorithm (22) was used to constrain all bond lengths involving hydrogen atoms. Optimization and relaxation of solvent and ions were initially performed, keeping the solute atoms constrained to their initial position with decreasing force constants of 500, 25, 15, and 5 kcal/(mol Å^2). The system has been simulated at a constant temperature of 300 K using Berendsen's method (23) and at a constant pressure of 1 bar with a 2-fs time step. Pressure and temperature coupling constants were 0.5 ps.

Table 1 shows the scheme of the different kinds of simulation carried out. Simulation A refers to the protein in the closed state without the DNA double strand and in the presence of 21 Cl^- counterions to neutralize the system (a total of 219 655 atoms, with 9415 protein atoms and 70 073 water molecules); in simulation B, the ionic strength has been increased introducing 21 atoms of Na^+ and 21 more Cl^- atoms (a total of 219 487 atoms, with 9415 protein atoms and 70 003 water molecules); in C, a positive charge value has been given to the lateral chain of the Glu 497 residue to introduce a repulsion with the close Lys369 in the opposite lip; in D, the repulsion between the two lips has been increased, introducing a positive charge value also to the main-chain carbonyl group of Glu497 and to the lateral chain carbonyl group of Asn366; in the final part of the simulation (simulation E), the charge perturbation was eliminated and an unperturbed simulation has been carried out for 10 ns.

The atomic RMSF have been computed by using the following definition:

$$\mathrm{RMSF}_i = \sqrt{\sum_{\alpha=1}^{3} \left\langle \left(r_{i,\alpha}^{\min}(t) - \bar{r}_{i,\alpha} \right)^2 \right\rangle_{\mathrm{MD}}}$$

where the averages have been computed over the equilibrated MD trajectory of simulation A, i.e. from 500 to 3500 ps.

The per-residue root mean square deviations (RMSDs) between two aligned structures X and Y have been computed by using the following definition:

$$\mathrm{RMSD}_{res}(X-Y)=\sqrt{\frac{1}{N_{\mathrm{res}}}\sum_{i=1}^{N_{\mathrm{res}}}\left|r_i^X-r_i^Y\right|^2}$$

where the distances between all atoms in a certain residue are averaged. The average per-residue RMSD for simulation E has been calculated by least-square fitting a group of main chain atoms to their initial position, calculating the per-residue RMSD with the previous equation, and averaging the resulting value on the entire 10 ns simulation time. All the analyses have been carried out using the GROMACS MD package version 3.3.1 (24). Figures 2, 4 and 5, and the movies of MD dynamics, shown as Supplementary Data at NAR Online, were created using the VMD visualization package (25).

Table 1. Conditions and lengths of the different simulations carried out for hTop1

Simulation	A	B	C	D	E
Charge perturbation	None		Glu497[b]	Glu497[a,b] and Asn 366[b]	None
Time (ps)	3500	500	200	200	10 000

[a]Main-chain perturbation.
[b]Side-chain perturbation.

RESULTS AND DISCUSSION

Initial unperturbed simulation

In the first 3500 ps of simulation in the absence of DNA, defined here as simulation A, the protein is maintaining a conformation very close to the crystallographic state, being the largest RMSD calculated on the main chain atoms of ~3.5 Å. This value is very close to that found for the protein simulated in complex with the DNA substrate for an identical simulation time length (13). This result indicates that the closed configuration of the protein is very stable, independently of the presence of DNA, and that the intra-domain and inter-domain protein interactions are sufficient to maintain the closed conformation. Also, the overall flexibility of the protein with or without DNA is quite similar, as can be observed in Figure 1, where the per-residue RMSF in the absence of DNA, evaluated for the last 3000 ps of simulation A, is compared to the RMSF evaluated on the same time window for the simulation previously carried out on the protein–DNA complex (13). The maxima and minima of the RMSF are identical in the two simulations, being very similar to the protein regions characterized by the largest flexibility. In fact, in the absence of DNA, the linker and the loop connecting β-strands 12 and 13 centered on Gly520 are the regions characterized by the largest fluctuations, as already observed for the enzyme in the closed

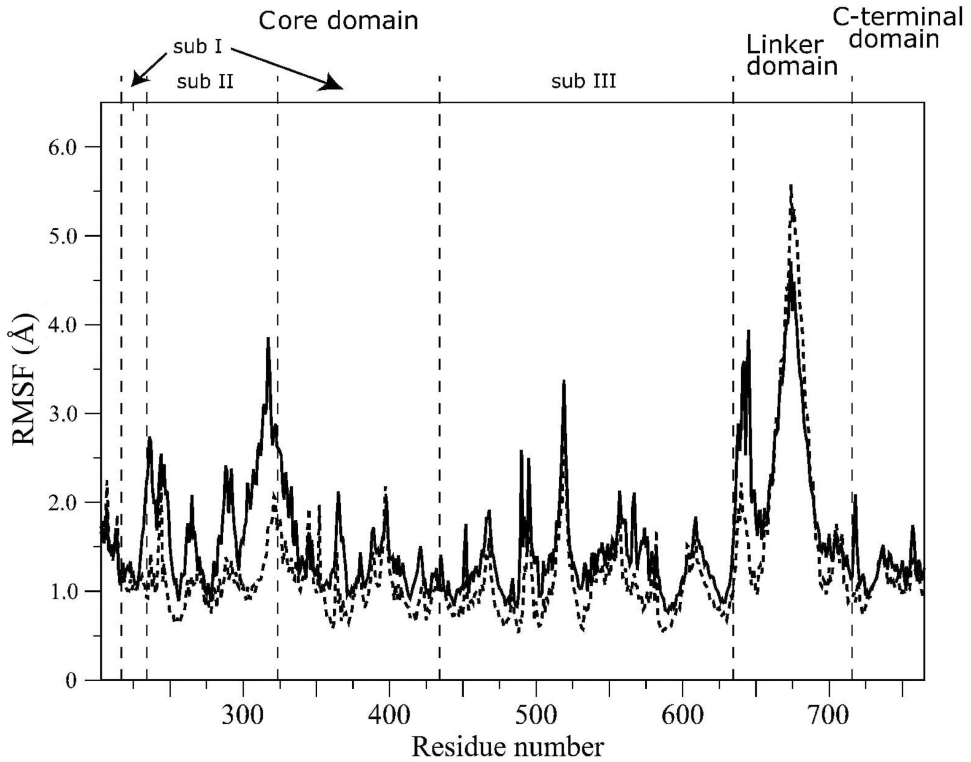

Figure 1. Average per-residue RMSF represented as a function of the residue number of hTop1 in the absence of DNA for the initial unperturbed simulation A (full line) in comparison with the ones previously calculated for the protein in complex with DNA (dashed line).

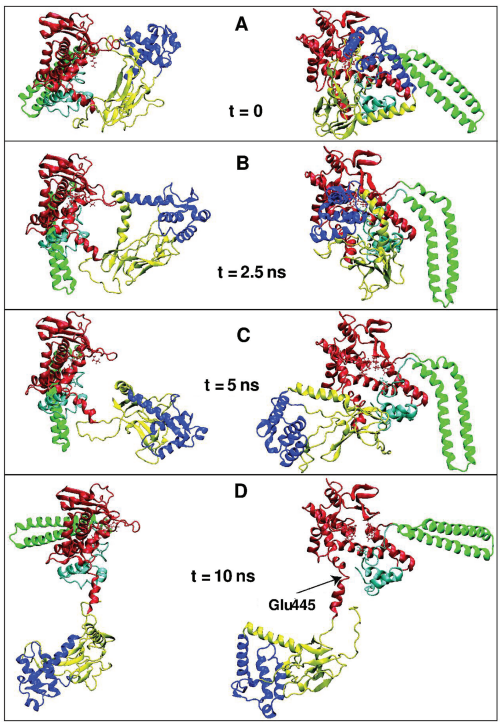

Figure 2. Four snapshots of the final unperturbed simulation E taken at different times, showing the opening of the protein. The snapshots are displayed in two different orthogonal orientations (left and right). Core subdomains I, II and III are rendered in yellow, blue and red, respectively. Linker and C-terminal domains are rendered in green and cyan, respectively. The five active site residues are represented in ball and stick. The hinge residue Glu445 is indicated by an arrow in panel D.

conformation in the presence of DNA (12). Differences are observed in the absolute values of the RMSF of definite regions, such as the 'nose-cone' helices (helices 5 and 6 in core subdomains II and I, respectively) and the small loop at the N-terminal of the linker domain (residues Pro636-Met645), which show larger RMSFs in the simulation without DNA than those observed in the simulation of topo70 in complex with DNA (Figure 1). Residues 634–640 are known to be highly flexible, and are not detected in several topoisomerase–DNA complex crystals because of their thermal fluctuations, while they are seen in the structure of the topo70–DNA–topotecan ternary complex (26). This region seems to display a scale of disorder, being more ordered in the ternary topo70–DNA–topotecan complex, less ordered in the binary topo70–DNA complex and even more disordered in the absence of DNA. On the contrary, the maximum fluctuations, located in the loop of the linker domain between helices 18 and 19, are less ample in the simulation without the DNA.

Per-residue-RMSDs (data not shown) give higher values in the simulation in the absence of DNA, for the linker domain and the nose-cone helices, which move away from the space previously occupied by DNA. Both these regions have been shown to form several direct and water-mediated contacts with the DNA phosphate groups in the strands downstream of the scissile base (5,11,13). It is worth noting, therefore, that the greater changes of dynamics and structure, in the absence of DNA but in the closed conformation, are located in the two regions involved in the controlling of the rotation of the scissile strand during the relaxation step.

An interesting difference is observed at the level of the inter-lip interactions. The X-ray diffraction study describes a single salt bridge direct contact between Lys369 and Glu497 (5). In the simulation in the absence of DNA, a new interaction is observed from ~900 and 2500 ps between the lateral chain of Lys369 and the carbonylic main-chain group of Glu497, with a distance of ~3 Å. After this time, the distance between these two groups increases to ~5 Å and the lateral chain of Asn366 and the Asp500 main chain start to interact, their distance being ~3 Å (see Figure 7, in Supplementary Data). It is interesting to note that this new inter-lip interaction is also observed in the last part (from ~1 to 3.5 ns) of the simulation of the protein in the presence of DNA (13).

Charge perturbation

A perturbation of the inter-lip interactions found at the end of simulation A, occurring between charged or polar groups ($Glu497COO^{-}$–$Lys369NH_3^{+}$; Glu497CO–$Lys369NH_3^{+}$; Asn366OD1–Asp500NH), has been attempted by increasing the ionic strength of the system. In details, 21 Na^{+} and Cl^{-} atoms have been added to the system, which has been simulated for 500 ps (simulation B).

However, since the energetic stability of the inter-lip interactions is not sufficiently perturbed by the increase of ionic strength (see Figure 7 in Supplementary Data), a not physical perturbation (i.e. change of electrostatic charges) has been introduced in the system, in order to create a destabilization within a simulation time compatible with the currently computational resources. It is interesting to note that the introduction of a positive charge replacing the negative one at the carboxylic group of Glu497 is not enough to push the two lips far away from each other. In fact, the introduction of the positive charge on the COO^{-} group of Glu497 leads to an increase of the Glu497–Lys369 distance because of electrostatic repulsion (black line in Figure 7 in Supplementary Data, simulation C). However, Lys369 changes its molecular partner and forms a strong interaction with the Glu497 main-chain carbonyl group, as evidenced by the decrease of the $CO - NH_3^{+}$ relative distance of the Glu497 main-chain and Lys369 lateral chain, respectively (red line in Figure 7 in Supplementary Data, simulation C). The same occurs for the interaction between the lateral chain of Asn366 and the main-chain of Asp500 (green line in Figure 7 in Supplementary Data). Therefore, the destabilization at the level of the salt bridge between Glu497 and Lys369 lateral chains, due to the introduction of the positive charge on the Glu497 lateral chain, is compensated for by the strengthening of other lip1–lip2 interactions that allow the protein to maintain a stable closed configuration. Only after the introduction of two additional positive charges, one on the carbonyl group of Glu497 and the other one on the lateral chain of Asn366, the two lips start to separate each other, as can be observed by monitoring the

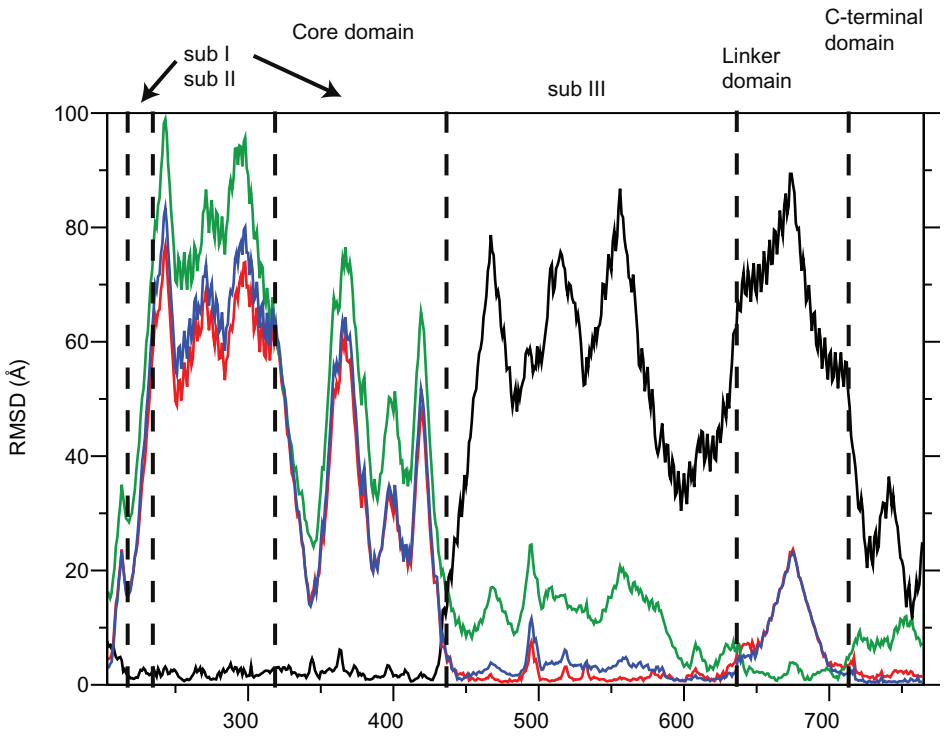

Figure 3. Average per-residue RMSD of hTop1 for the final unperturbed simulation E represented as a function of the residue number. The average per-residue RMSD have been calculated overlapping the protein on the initial position of the core subdomains I and II (black line), the core subdomain III (red line), the linker (green line) or the C-terminal domain (blue line).

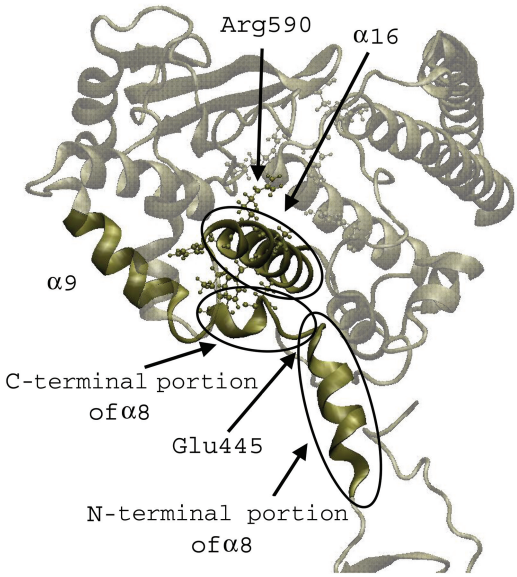

Figure 4. Snapshot of the final configuration of simulation E, showing only the core subdomain III, the C-terminal, and the linker domain regions of the protein. Helices 8, 9 and 16 and the catalytic Arg590 are highlighted in the figure to evidentiate the hydrophobic interactions between the C-terminal portion of helix 8 and helix 16. The hinge residue Glu445 is also indicated by an arrow.

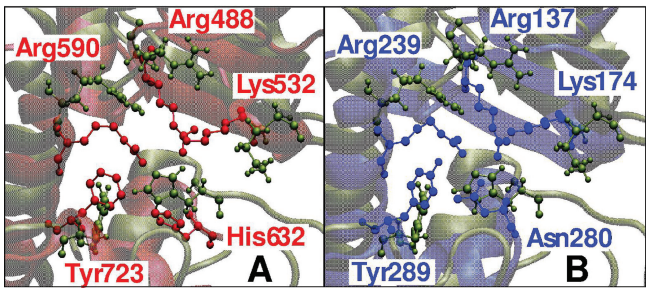

Figure 5. (**A**) superimposition of the active site region of the last frame of simulation E (gray color) with the human enzyme X-ray structure (red color). (**B**) Superimposition of the active site region of the last frame of simulation E (gray color) with the *Deinococcus radiodurans* enzyme X-ray structure (blue color).

above-mentioned distances in simulation D (Figure 7 in Supplementary Data).

The system has been allowed to evolve with this additional perturbation for 200 ps. After this time, the positive charges have been eliminated, bringing the modified residues charges back to their initial values. The minimum distance between the lips, in the first configuration of the following unperturbed simulation (simulation E), is only 6.5 Å, and the overall RMSD of this structure is 3.5 Å from the initial X-ray configuration (deviation of the main-chain atoms fitted on the main-chain atoms themselves).

Opening dynamics

The initial configuration and three significant snapshots taken from simulation E are shown in Figure 2. A dynamic visualization of the MD dynamics is available as Supplementary Data at NAR Online. The first

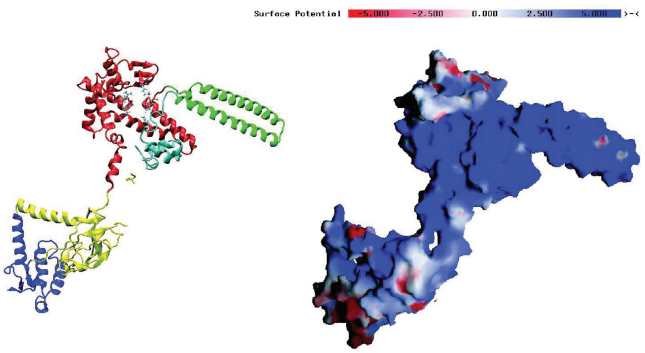

Figure 6. A snapshot of the open conformation of the final unperturbed simulation E represented with the same domain colors as Figure 2 (left panel), together with its electrostatic potential mapped onto its molecular surface (right panel). Red color represents negative and blue positive potential (−5 to +5 k_BT). Electrostatic potentials were calculated using the program GRASP (29).

important observation is that the protein domains change their relative position, reaching an open conformation able to bind and trap the DNA substrate, but the secondary and tertiary structures of the single domains are very well conserved during the entire simulation period. This is an important observation, since it implies that the different domains act as independent and internal coherent units that maintain their overall structure, although strongly changing their relative orientation. Core subdomains I and II (colored yellow and blue, respectively) show coordinated motion, separated from that of core subdomain III (colored red). This last subdomain, on the other hand, remains strongly interacting with the C-terminal domain (colored cyan) throughout the simulation. A quantitative analysis of the relative protein domain motion is represented in Figure 3, where the average per-residue RMSD has been calculated, overlapping the protein on the core subdomains I and II (black line), the core subdomain III (red line), the linker (green line), or the C-terminal domain (blue line). The analysis indicates a very strong and coherent motion of the core subdomains I–II with respect to the other protein domains, with maximum RMSD (about 100 Å) when the protein is fitted on the linker domain. Figure 2 helps to understand this huge relative motion. The destabilization of the lip interactions permits a rotation of the core subdomains I–II nose-cone helices, initially orientated parallel to the linker domain (Figure 2A), of nearly 90° after 2.5 ns (Figure 2B) and of ~180° after 5 ns (Figure 2C). This motion permits the opening of the two halves that embrace the DNA, formed by core subdomains I–II on one side and core subdomain III and C-terminal domain on the other side. The strong movement of core subdomains I–II continues during the last 5 ns of the simulation time, although with a lower extent. The region that permits these relative domain motions is the N-terminal portion of helix 8 (residues 434–444, Figures 2D and 4), and can be identified also by the intersection of the black and red lines in Figure 3. Glu445 behaves as the hinge residue (Figures 2D and 4). The C-terminal portion of helix 8, on the contrary, remains strongly interacting with helix 16 located in the C-terminal domain, during the whole opening dynamics (Figure 4). These two regions remain in close contact because of the presence of a cluster of hydrophobic residues. On the opposite site of this portion of helix 16 is located Arg590, a residue belonging to the catalytic pentad (27) that, due to these hydrophobic interactions, is maintained in an orientation similar to the one found in the crystallographic structures. Actually, all five active site residues maintain, for the whole simulation time, an orientation very similar to the one found in the closed configuration detected through X-ray diffraction (5). The similar orientation can be appreciated in Figure 5A where the active site region of the last frame of simulation E (gray) is overimposed on the X-ray structure (red). As a matter of fact, the largest deviation of the active site backbone atoms from the 1a36 crystallographic structure is only 1.7 Å. The recent 3D structure of *Deinococcus radiodurans* (DRA) topoisomerase IB, the only one crystallized in an open conformation in the absence of DNA, has indicated that the five active site residues are preassembled, being in a position nearly identical to those found in the DNA-bound human hTop1 (10). In line, the orientation of the active site residues of the human enzyme in our simulation is also very similar to that of the bacterial enzyme, as shown in Figure 5B, where the last frame of simulation E (gray) is overimposed to the structure of DRA (blue).

In our simulation, despite the huge inter-domain protein motion that spans up to 100 Å, the active site residues fully maintain their relative orientation, indicating that, in the human enzyme also, the active site is preassembled and in the appropriate position to cleave the DNA substrate, at variance with what has been proposed for the vaccinia virus enzyme, where only the DNA binding would trigger the active site assembly (28). The presence of a preassembled active site suggests that, in the open conformation, the enzyme is ready to interact with DNA, and the only conformational change that the protein must undergo is the one needed to embrace the substrate. In line, electrostatic calculation of the open protein conformation shows that the protein displays a vast positive region (blue in Figure 6) with the active site resides located nearly at its center, perfectly suited to interact with the negatively charged supercoiled DNA substrate.

SUPPLEMENTARY DATA

Supplementary Data are available at NAR Online.

ACKNOWLEDGEMENTS

The authors thank J.Z. Pedersen for the critical reading of this article. We acknowledge the CASPUR Computational Center for the computer architecture used in this work. This work was partly supported by grants from COFIN2005 and by an FIRB project on Bioinformatics for Genomics and Proteomics. Funding to

pay the Open Access publication charges for this article was provided by a grant from COFIN2005 to A.D.

Conflict of interest statement. None declared.

REFERENCES

1. Chen,A. and Liu,L.F. (1994) DNA topoisomerases: essential enzymes and lethal targets. *Ann. Rev. Pharmacol. Toxicol.*, **34**, 191–218.
2. Nitiss,J. (1998) Investigating the biological functions of DNA topoisomerases in eukaryotic cells. *Biochem. Biophys. Acta.*, **1400**, 63–82.
3. Wang,J.C. (1996) DNA topoisomerases. *Ann. Rev. Biochem.*, **65**, 635–692.
4. Stewart,L., Ireton,G.C. and Champoux,J.J. (1996) The domain organization of human topoisomerase I. *J. Biol. Chem.*, **271**, 7602–7608.
5. Redinbo,M.R., Stewart,L., Kuhn,P., Champoux,J.J. and Hol,W.G.J. (1998) Crystal structures of human topoisomerase I in covalent and noncovalent complexes with DNA. *Science*, **279**, 1504–1513.
6. Stewart,L., Redinbo,M.R., Qiu,X., Hol,W.G.J. and Champoux,J.J. (1998) A model for the mechanism of human topoisomerase I. *Science*, **279**, 1534–1541.
7. Sari,L. and Andricioaei,I. (2005) Rotation of DNA around intact strand in human topoisomerase I implies distinct mechanisms for positive and negative supercoil relaxation. *Nucleic Acids Res.*, **33**, 6621–6634.
8. Woo,M.H., Losasso,C., Guo,H., Pattarello,L., Benedetti,P. and Bjornsti,M.-A. (2003) Locking the DNA topoisomerase I protein clamp inhibits DNA rotation and induces cell lethality. *Proc. Natl Acad. Sci.*, **100**, 13767–13772.
9. Carey,J.F., Schultz,S.J., Sisson,L., Fazzio,T.G. and Champoux,J.J. (2003) DNA relaxation by human topoisomerase I occurs in the closed clamp conformation of the protein. *Proc. Natl. Acad. Sci.*, **13**, 5640–5645.
10. Patel,A., Shuman,S. and Mondragon,A. (2006) Crystal structure of a bacterial type IB DNA topoisomerase reveals a preassembled active site in the absence of DNA. *J. Biol. Chem.*, **281**, 6030–6037.
11. Chillemi,G., Castrignano,T. and Desideri,A. (2001) Structure and hydration of the DNA-human topoisomerase I covalent complex. *Biophys. J.*, **81**, 490–500.
12. Chillemi,G., Fiorani,P., Benedetti,P. and Desideri,A. (2003) Protein concerted motions in the DNA-human topoisomerase I complex. *Nucleic Acids Res.*, **31**, 1525–1535.
13. Chillemi,G., Redinbo,M.R., Bruselles,A. and Desideri,A. (2004) Role of the linker domain and the 203-214 N-terminal residues in the human topoisomerase I DNA complex dynamics. *Biophys. J.*, **87**, 4087–4097.
14. Chillemi,G., Fiorani,P., Castelli,S., Bruselles,A., Benedetti,P. and Desideri,A. (2005) Effect on DNA relaxation of the single Thr718Ala mutation in human topoisomerase I: a functional and molecular dynamics study. *Nucleic Acids Res.*, **33**, 3339–3350.
15. Bockmann,R.A. and Grubmuller,H. (2002) Nanoseconds molecular dynamics simulation of primary mechanical energy transfer steps in F1-ATP synthase. *Nat. Struct. Biol.*, **9**, 198–202.
16. Moonsoo,J., Andricioaei,I. and Springer,T.A. (2004) Conversion between three conformational states of integrin I domains with a C-terminal pull spring studied with molecular dynamics. *Structure*, **12**, 2137–2147.
17. Redinbo,M.R., Champoux,J.J. and Hol,W.G. (2000) Novel insights into catalytic mechanism from a crystal structure of human topoisomerase I in complex with DNA. *Biochemistry*, **39**, 6832–6840.
18. Cornell,W.D., Cieplak,P., Bayly,C.I., Gould,I.R., Merz,K.M.Jr, Ferguson,D.M., Spellmeyer,D.C., Fox,T., Caldwell,J.W. *et al.* (1995) A second generation force field for the simulation of proteins, nucleic acids and organic molecules. *J. Am. Chem. Soc.*, **117**, 5179–5197.
19. Jorgensen,W.L., Chandrasekhar,J., Madura,J.D., Impey,R.W. and Klein,M.L. (1983) Comparison of simple potential functions for simulating liquid water. *J. Chem. Phys.*, **79**, 926–935.
20. Darden,T., York,D. and Pedersen,L. (1993) Particle mesh Ewald-an N.log(n) method for Ewald sums in large systems. *J. Chem. Phys.*, **98**, 10089–10092.
21. Cheatham,T.E., Miller,J.L., Fox,T., Darden,T.A. and Kollman,P.A. (1995) Molecular dynamics simulation on solvated biomolecular systems: the particle mesh Ewald method leads to stable trajectories of DNA, RNA, and proteins. *J. Am. Chem. Soc.*, **117**, 4193–4194.
22. Ryckaert,J.-P., Ciccotti,G. and Berendsen,H.J.C. (1977) Numerical integration of the Cartesian equations of motion of a system with constraints: molecular dynamics of n-alkanes. *J. Comput. Phys.*, **23**, 327–341.
23. Berendsen,H.J.C., Postma,J.P.M., van Gusteren,W.F., Di Nola,A. and Haak,J.R. (1984) Molecular dynamics with coupling to an external bath. *J. Comput. Phys.*, **81**, 3684–3690.
24. van der Spoel,D., Lindahl,D., Hess,B., Groenhof,G., Mark,A.E. and Berendsen,H.J.C. (2005) GROMACS: fast, flexible and free. *J. Comp. Chem.*, **26**, 1701–1718.
25. Humphrey,W., Dalke,A. and Shulten,K. (1996) VMD-visual molecular dynamics. *J. Mol. Graph.*, **14**, 33–38.
26. Staker,B.L., Hjerrild,K., Feese,M.D., Behnke,C.A., Burgin,A.B. and Stewart,L. (2002) The mechanism of topoisomerase I poisoning by a camptothecin analog. *Proc. Natl. Acad. Sci.*, **99**, 15387–15392.
27. Leppard,J.B. and Champoux,J.J. (2005) Human DNA topoisomerase I: relaxation, roles, and damage control. *Chromosoma*, **114**, 75–85.
28. Tian,L., Claeboe,C.D., Hecht,S.M. and Shuman,S. (2004) Remote phosphate contacts trigger assembly of the active site of DNA topoisomerase IB. *Structure*, **12**, 31–40.
29. Nicholls,A., Sharp,K.A. and Honig,B. (1991) Protein folding and association: insights from the interfacial and thermodynamic properties of hydrocarbons. *Proteins*, **11**, 281–296.